Renewable fuel production from hydropyrolysis of residual biomass using molybdenum carbide-based catalysts: An analytical Py-GC/MS investigation

Marta A. Machado[a], Songbo He[b], Thomas E. Davies[c], K. Seshan[b], Victor Teixeira da Silva[a,]

[a] Universidade Federal do Rio de Janeiro, Programa de Engenharia Química – COPPE, P.O. Box 68502, 21941-914, RJ, Rio de Janeiro, Brazil
[b] Catalytic Processes and Materials, Faculty of Science & Technology, University of Twente, 7500 AE, Enschede, The Netherlands
[c] Cardiff Catalysis Institute, School of Chemistry, Cardiff University, Main Building, Park Place, CF10 3AT, Cardiff, United Kingdom

ARTICLE INFO

Keywords:
Renewable fuels
Molybdenum carbide
Hydropyrolysis
Hydrodeoxygenation
Py-GC/MS

ABSTRACT

Fast hydropyrolysis of lignocellulosic biomass was studied by using an analytical pyrolyzer coupled with a gas chromatography/mass spectrometry set-up (Py-GC/MS). Under pure H_2 stream, Canadian pinewood was rapidly heated up to 500 °C and the generated vapors passed through a catalytic bed at 500 °C. Experiments were carried out in order to compare the catalytic performance of MoC/Al_2O_3 catalyst to a reference catalyst based on noble metal (1.5 wt.% Pt/Al_2O_3). The effect of different supports (Al_2O_3, ZrO_2 and MgO) on the carbide performance and product formation was investigated. The results showed that the performance of MoC/Al_2O_3 was similar to that of 1.5 wt.% Pt/Al_2O_3. Both of them deoxygenated the hydropyrolysis vapors and led exclusively to hy-drocarbons formation. However, the proportion of aliphatic and aromatic hydrocarbons was different: MoC/ Al_2O_3 catalyst produced more aliphatics (57%) than the Pt catalyst. The supports have demonstrated influence on the product distribution. Acidity of the support seems to play an important role in the deoxygenation of the vapors. While there was complete removal of oxygen when MoC/Al_2O_3 and MoC/ZrO_2 were used, the same did not take place for the more basic MoC/MgO catalyst.

1. Introduction

It is a well-known fact that the intensive use of fossil fuels in the last decades has brought about economic, political and environmental concerns. In this way, great technological development efforts are being devoted toward their partial replacement by renewable and econom-ically sustainable energy sources. Considering this, biomass appears as an alternative for producing fuels and chemicals once it has been la-beled as the unique available sustainable source of organic carbon. Due to its abundant supply and non-competition with food crops, residual lignocellulosic biomass derived either from agricultural wastes or wood processing has been intensively studied as potential source of renew-able biofuels [1,2].

Fast pyrolysis is considered a promising technique for lig-nocellulosic biomass conversion into liquid fuels. This method is based on thermal decomposition of raw biomass in an oxygen- free atmo-sphere at moderate temperatures (~500 °C) by using high heating rates (10^4 °C s^{-1}) and short vapor residence times (< 2 s). The rapid cooling of the generated vapors leads to the formation of a dark brown liquid product, denominated bio-oil, which can reach yields around 70 wt.% [3,4].

Bio-oil is a complex mixture of oxygenated organic molecules with undesired properties such as low energy content, acidity, high viscosity and chemical instability. For instance, the presence of carboxylic acids and carbonyl compounds (aldehydes and ketones) leads to a corrosive nature and instability of the oil, respectively. Thus, the direct applica-tion of bio-oil as fuel shows several restrictions [3].

The upgrading of bio-oil can be achieved by reducing its oxygen content via deoxygenation reactions such as decarbonylation, dec-arboxylation, direct deoxygenation (hydrogenolysis), dealkoxylation, cracking, hydrocracking, hydrogenation, dealkylation, methyl transfer and hydrodeoxygenation reactions. Amongst them, the last one is the preferred route in the upgrading process once the oxygen is removed as H_2O resulting in enhancement of liquid yields and no loss of carbon [5].

In order to promote bio-oil hydrodeoxygenation (HDO), many stu-dies found in the literature make use of traditional hydrotreating cat-alysts based on sulfides, temperatures around 300–500 °C and an ex-ternal source of hydrogen [5,6]. The use of sulfides must be avoided because some sulfur can be leached from the active phase and react with the molecules in the feed thus ending up in the final product, which is undesirable. Moreover, sulfur leaching leads to catalyst de-activation. Although noble metal catalysts can be also applied in

Corresponding author.
E-mail address: victor.teixeira@peq.coppe.ufrj.br (V. Teixeira da Silva).

hydrotreating [3,5,7], the use of precious metals increases the final production costs [8]. A cheaper alternative is their replacement by transition metal carbides, which have catalytic behavior comparable to noble metal catalysts and are sulfur resistant [9].

Most of the works adopting transition metal carbides for biomass upgrading make use of model compounds as reactant in order to un-derstand the chemical steps involved in the mechanism of deoxygena-tion [5,10–18]. There are few studies using carbides in the upgrading of raw bio-oil. In one of them, Patel et al. [19] have investigated the fast pyrolysis of sugarcane bagasse in a fluidized bed reactor utilizing 20 wt.

% Mo_2C/Al_2O_3 as catalyst. The authors have observed the reduction of sugars while the amounts of furanic and phenolic compounds have increased. However, no deoxygenation products were detected prob-ably due to the utilization of nitrogen as the fluidizing agent instead of hydrogen. In another study, Choi et al. [20] evaluated a series of metal-doped bulk Mo carbide in the hydroprocessing of pine-derived bio-oil. Results showed that the presence of catalysts promoted the formation of hydrocarbons and the removal of oxygenated compounds, reaching an oxygen content reduction of 94% for the Ni-doped bulk Mo_2C catalyst. Remarkably, this bulk carbide catalyst could be easily regenerated after deactivation. Nonetheless, the problem of the use of pyrolysis oil as a reactant for upgrading is the presence of reactive molecules in the bio-oil that can in parallel undergo polymerization and increase the average molecular weight, which causes lower reactivity for hydrodeoxygena-tion [7].

Usually, fast pyrolysis of the biomass takes place in an inert atmo-sphere (N_2, Ar or He). However, the thermal decomposition in the presence of H_2 can allow the reaction between the volatile organic products and hydrogen. Although, literature reports that the use of H_2 in a fast pyrolysis system does not lead to an extensive deoxygenation degree at low pressures, the addition of catalysts to the upgrading process have shown promise. The association between fast pyrolysis carried out in a reducing atmosphere and catalytic upgrading of pyr-olysis vapors leads to the concept of catalytic fast hydropyrolysis [21].

The main objective of this work was to evaluate the performance of supported molybdenum carbide catalysts in the deoxygenation of hy-dropyrolysis vapors of pinewood using a pyrolyzer-gas chromato-graphy/mass spectrometry (Py-GC/MS) system. Three diff erent oxides (Al_2O_3, ZrO_2 and MgO) were used as supports for molybdenum carbide in order to verify their eff ect on the overall distribution of the GC-vo-latile products. These materials were chosen due to their distinct acid-base properties.

2. Materials and methods

2.1. Catalyst preparation

γ-Al_2O_3 (Alfa Aesar 43832), ZrO_2 (Gimex Technisch Keramik B.V. RC100) and MgO (Merck 105867) were used as supports for mo-lybdenum carbide. The precursors were synthesized by incipient wet-ness impregnation method using an aqueous solution of ammonium heptamolybdate ($(NH_4)_6Mo_7O_{24}{\cdot}4H_2O$, Sigma Aldrich) in order to ob-tain a carbide loading of 20 wt.%, followed by calcination at 500 °C (heating rate of 5 °C min^{-1}) for 5 h. The synthesized precursors 26 wt.

% MoO_3/X (X = Al_2O_3, ZrO_2 or MgO) were then carburized by means of temperature-programmed carburization (TPC) method. 100 mg of each sample was heated from room temperature up to 650 °C (heating

rate of 2.5 °C min^{-1}) under a stream of 20 vol.% CH_4/H_2 (100 mL min^{-1}). The temperature was kept isothermal at 650 °C for 2 h before cooling down to room temperature. The use of these conditions allows the production of "clean" Mo_2C, i.e. Mo_2C without any carbon contamination due to thermal decomposition of methane as shown in literature [22,23]. As transition metal carbides are pyrophoric, an ad-ditional step of passivation was needed in order to avoid bulk oxidation after their exposure to the atmosphere. Therefore, all samples were passivated under a stream of 1 vol.% O_2/N_2 (30 mL min^{-1}) overnight.

For comparison purposes, a platinum catalyst supported on γ-Al_2O_3 (1.5 wt.% Pt/Al_2O_3) was prepared as described elsewhere [24].

2.2. Catalyst characterizations

MoO_3 loadings were determined by using X-ray fluorescence tech-nique (XRF; Philips, PW1480).

X-ray diffraction (XRD) patterns were recorded on a Rigaku Rix 3100 instrument with a Cu Kα radiation at 30 kV and 15 mA. The analyses were carried out in the 2θ range from 5 to 90° at speed of 2° per minute.

CO uptake measurements were carried out in situ immediately after TPC method by pulsing calibrated volumes of a 20 vol.% CO/He gas mixture at room temperature and acquiring online the ion signal m/ z = 28 with a mass spectrometry (Pfeiffer Vacuum, model D-35614 Asslar).

The specific surface area values were obtained by N_2 physisorption at −196 °C. The values were calculated by B.E.T. method using a single point (P/P_0 = 0.3). The analyses were carried out in situ and a complete description of the experimental procedure can be found in reference [25].

The total acid sites of reactivated carbide catalysts and pure sup-ports were quantified by adsorption of a 4 vol.% NH_3/He gas mixture at room temperature. Prior to the experiment, the passivated carbide was reactivated in situ at 500 °C (heating rate of 10 °C min^{-1}) under flow of pure H_2 during 60 min. The ion signals m/z = 17 and m/z = 15 were monitored online by means of a mass spectrometry (Pfeiffer Vacuum, model D-35614 Asslar). The experimental procedure to determine the total quantity of chemisorbed NH_3 matter was based on a dynamic method described in the Supplementary information.

2.3. Hydropyrolysis reaction

Fast hydropyrolysis experiments were carried out in a Pyroprobe® 5200 pyrolyzer (CDS Analytical) at atmospheric pressure. Approximately, 500 μg of biomass (Canadian pinewood) was loaded in a quartz tube reactor that was heated up to 500 °C at a heating rate of 20 °C ms^{-1} under a flow of pure H_2 (15 mL min^{-1}). The pyrolysis va-pors exiting the reactor passed through a catalytic fixed-bed reactor (3 mg of catalyst mixed with 3 mg of quartz sand) kept at 500 °C. All of the products were analyzed by an on-line GC/MS (Agilent, model 6890N-5975) equipped with a capillary column (Agilent VF–1701 ms, 60 m length, 0.25 mm i.d., 0.25 μm film). Helium was used as carrier gas at a flow rate of 1.2 mL min^{-1}. The analyses were done using the following temperature profile: 40 °C for 5 min, raised up to 280 °C at 3 °C min^{-1}, held at 280 °C for 10 min. The mass spectrum of all de-tected products was obtained at 70 eV (ionization energy) using the scan mode (from m/z = 25 to m/z = 550). The identification of com-pounds was based on the obtained mass fragmentation patterns ac-quired by the coupled mass spectrometer using peak matching of cor-responding chromatographic peaks with those of NIST database.

Before hydropyrolysis, passivated carbides were reactivated (and Pt/Al_2O_3 catalyst was reduced) in situ at 500 °C under pure H_2 stream for 30 min. Besides, the bulk MoO_3 precursor was also tested and it was pretreated in situ at 500 °C under pure He stream for 30 min.

Each reaction was performed at least three times to check experi-mental reproducibility and calculate the confidence interval, con-sidering a confidence level of 95%.

As it is known, the use of Py-GC/MS system does not provide a fully quantitative analysis with high accuracy due to the complex nature of the bio-oil and the lack of commercial standards. However, many re-searchers have already proposed to apply a semi-quantitative analysis using the peak area percentage [26–30]. This relies on the fact that variations in the chromatographic peak area of a component are con-sidered linear with the variations of its quantity. Accordingly, varia-tions in the peak area percentage of this component is linear with the

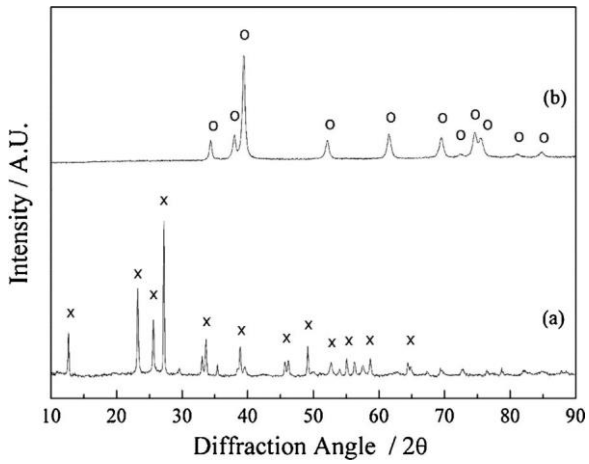

Fig. 1. XRD patterns of bulk MoO_3 (a) and bulk Mo_2C (b). The crosses and circles re-present the characteristic diffraction peaks of MoO_3 (JCPDS 05-0508) and Mo_2C (JCPDS 35-0787), respectively.

variations of its concentration. Considering that all experiments were carried out using the same type and mass of feedstock, the comparison of the peak area percentages are suitable

The compounds identified by GC/MS were grouped as acids, car-bonyls, furans, phenols, aliphatic hydrocarbons (HC), aromatic HC, alcohols and miscellaneous (misc.).

3. Results and discussion

3.1. Catalyst characterizations

The XRD patterns of bulk MoO_3 and bulk Mo_2C synthesized by TPC are shown in Fig. 1(a-b). According to Joint Committee on Powder Diffraction Standards (JCPDS) database, both samples presented their characteristic diffraction patterns. MoO_3 exhibited the main diffraction peak at $2\theta = 27.4°$, corresponding to the (0 4 0) plane of an orthor-hombic unit cell (JCPDS 05-0508). For bulk Mo_2C, the position of the highest relative intensity was at $2\theta = 39.4°$, ascribed to the (0 1 0) plane of a hexagonal close packed unit cell (β-Mo_2C crystalline phase) (JCPDS 35-0787).

Theoretically, to achieve a Mo_2C loading of 20 wt.% in a supported catalyst, the precursor should have a MoO_3 loading of 26 wt.%. Considering the theoretical and real results obtained from XRF pre-sented in Table 1, it is possible to conclude that the catalyst synthesis was performed in a proper way, once the real loadings are close to the nominal ones for all of the synthesized samples.

Independently of the support, the high loadings of molybdenum oxide led to the formation of crystallites observable by XRD, as can be seen in Fig. 2(a). However, after the carburization step, it was not possible to identify any of the diffraction lines related to β-Mo_2C (vertical dotted line in Fig. 2(b)). Only the diffraction peaks of the supports (γ-Al_2O_3 at $2\theta = 36.8°$, 45.5° and 66.5°; monoclinic ZrO_2 at $2\theta = 24.2°$, 28.2°, 31.5°, 34.2°, 35.3°, 40.7° and 50.1°; cubic MgO at $2\theta = 36.8°$, 42.8°, 62.2°, 74.5° and 78,4°) were identified, as can be seen in Fig. 2(b). Thus, the absence of characteristic diffraction peaks of β-Mo_2C in the supported samples might indicate the formation of very small particles highly dispersed and presenting crystallite sizes below the detection limit. In fact, HRTEM micrographs presented in the Supplementary Information (please see Figs. S2, S3 and S4) show that the observed particles have sizes in the range from 1 to 5 nm after the carburization step.

Table 1
MoO_3 loading in the different samples determined by XRF.

Sample	MoO_3 loading (wt.%)
MoO_3/Al_2O_3	27.3
MoO_3/ZrO_2	26.9
MoO_3/MgO	27.4

Despite the fact that was not possible to pinpoint the exact nature of the formed phase after the carburization step, a proof that the original molybdenum oxide species were transformed into carburized species (hereafter referred as MoC/X, X = Al_2O_3, ZrO_2 or MgO) is given by the CO uptake results presented in Table 2, where neither the oxidic sam-ples nor the support chemisorb this probe molecule.

The specific surface area (S_g) values of the supports (X = Al_2O_3, ZrO_2 and MgO), precursors (26 wt.% MoO_3/X) and catalysts (bulk Mo_2C and MoC/X) are presented in Table 2. It can be observed that the specific areas of the MoO_3/X samples were lower than those of the corresponding supports, as expected. It is known that bulk MoO_3 has a low specific area ($S_g < 10$ m^2 g^{-1}) [31]. Therefore, the decrease in the S_g value was coherent with the MoO_3 content, corresponding to 26% of the support total area. After the carburization, the supported carbides showed an increase of the specific area value if compared to their precursors. Bulk Mo_2C presents a considerably higher value compared to that of bulk MoO_3.

From the ammonia uptake showed in Table 2, it is possible to conclude that the acidity of the supports follows the order MgO < ZrO_2 < Al_2O_3, which is in agreement with the literature [32]. Bulk Mo_2C presented a significant NH_3 uptake (58 μmol g^{-1}), in accordance to the previous re-sults demonstrated by Bej et al. [33]. It is noteworthy that MoC/Al_2O_3 catalyst presents more acid sites (250 μmol of NH_3 g^{-1}) than the sum of the individual contributions of Mo_2C (0.2 × 58 = 11.6 μmol of NH_3 g^{-1}) and Al_2O_3 (0.8 × 136 = 108.8 μmol of NH_3 g^{-1}). This result can be ex-plained considering that while bulk Mo_2C presents big particles, when supported the carbide is in a highly-dispersed form, which leads to the formation of more acid sites.

3.2. Hydropyrolysis of biomass

The hydropyrolysis of Canadian pinewood was carried out in a Py-GC/MS set-up which can only be conducted in batch mode. It is im-portant to highlight that this type of system shows some drawbacks that should be addressed. The main one concerns the reaction products which cannot be collected due to the extremely low quantity (~500 μg) of the feedstock employed in the experiments. For this reason, it is not possible to obtain the mass balance and to monitor the gas phase. However, a previous report in the literature [34] has proven that the composition of volatile pyrolysis products obtained from Py-GC/MS and a bench-scale pyrolyzer is in close agreement. This result reveals that Py-GC/MS can be successfully used as a qualitative technique to screen catalysts and to indicate the nature of the formed products.

The first set of experiments consisted to perform the thermal hy-dropyrolysis without catalyst, in order to evaluate the organic mole-cules which will be catalytically upgraded later. In this experiment, more than 100 compounds were detected by GC/MS, as can be ob-served in a typical chromatogram showed in Fig. S5 (Supplementary information). It is noteworthy that this analysis method only captures the volatile products. However, it is important to be aware that there is also the formation of bio-char, lights gases and a portion of tar which were not analyzed in this work.

Due to the large number of products obtained during the thermal experiment, Table 3 lists only the compounds with chromatographic peak area percentages higher than 1%. A variety of oxygenated com-pounds were produced including simple molecules (such as carboxylic acids, ketones, aldehydes, alcohols and esters), furanics and sugars, which come from the decomposition of cellulose and hemicellulose, as well as phenolic compounds derived from lignin (such as phenols, cresols and guaiacols). Acetic acid has shown the largest peak area percentage suggesting that this was the major product from the reac-tion. Its formation can take place by different routes, being the

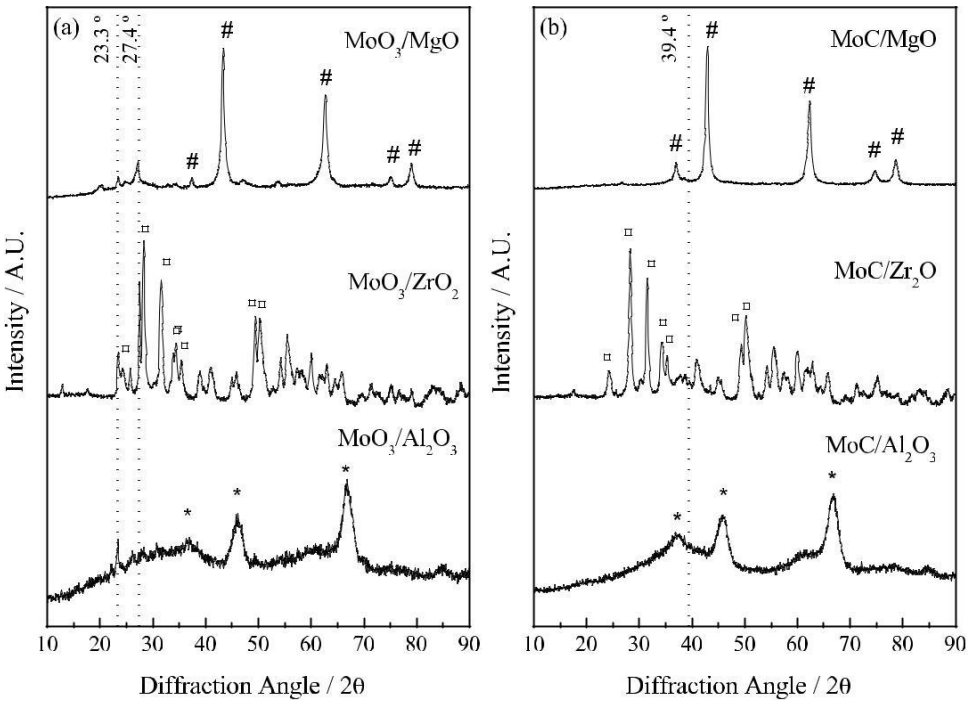

Fig. 2. XRD patterns of 26 wt.% MoO_3/Al_2O_3, 26 wt. % MoO_3/ZrO_2 and 26 wt.% MoO_3/MgO (a) and MoC/Al_2O_3, MoC/ZrO_2 and MoC/MgO (b). The asterisks, squares and hashes represent the character-istic diffraction peaks of γ-Al_2O_3 (JCPDS 47-1770), monoclinic ZrO_2 (JCPDS 37-1484) and cubic MgO (JCPDS 45-0946), respectively. On the left panel, the vertical dotted lines represent the characteristic diffractions of MoO_3. On right panel, the vertical dotted line at 39.4° represents the diffraction angle of the (0 1 0) plane of β-Mo_2C.

Table 2
Specific surface area (S_g), CO uptake and NH_3 uptake of supports, precursors and cata-lysts.

Sample	S_g ($m^2\ g^{-1}$)	CO uptake (μmol g^{-1})	NH_3 uptake (μmol g^{-1})
Bulk Mo_2C	94	62	58
Al_2O_3	200	0	136
MoO_3/Al_2O_3	150	0	–
MoC/Al_2O_3	174	179	250
ZrO_2	61	0	20
MoO_3/ZrO_2	43	0	–
MoC/ZrO_2	66	106	121
MgO	75	0	0
MoO_3/MgO	59	0	–
MoC/MgO	79	118	79

– It was not measured.

deacetylation of hemicellulose the most likely one [26]. Regarding the phenolic compounds, it is well-known that lignin can undergo de-methoxylation, demethylation and alkylation reactions. Demethoxyla-tion reactions can form compounds such as phenol, guaiacol and 4-ethylphenol, whereas demethylation and alkylation reactions can pro-duce catechol and o-cresol, respectively [26].

In order to deoxygenate the organic volatile molecules formed during thermal hydropyrolysis, a set of catalyst samples were tested one-by-one. Regarding to the upgrading experiments, it is relevant to emphasize the importance of biomass-to-catalyst ratio on the product distribution. It is reported in the literature [30,35,36] that low ratios (< 0.2) lead to high deoxygenation extension. On the other hand, ratios higher than 0.3 favor oxygenated compounds formation, such as car-boxylic acids, furans, phenols and cresols. Taking into consideration that this work aimed at forming compounds with low oxygen content, all experiments were undertaken at a biomass-to-catalyst ratio of 0.17, in order to perform an efficient deoxygenation and maximize the for-mation of hydrocarbons.

Fig. 3 compares the product distribution of thermal experiment with the results achieved by using bulk Mo_2C and its respective oxide, as well is also observed in Table 4. As can be seen, the non-catalytic hydro-pyrolysis led to generation of high amounts of oxygenates including 9% of acids, 38% of carbonyl containing compounds, 12% of furans and

Table 3
Compounds produced during biomass thermal hydropyrolysis.

Retention time (min)	Compound	Chromatographic peak area%
4.355	Acetaldehyde	3.9
5.052	Acetone	4.6
5.183	Propyl acetate	3.1
6.589	2,3-Butanedione	3.1
7.615	Acetaldehyde, hydroxy	1.2
8.701	Acetic acid	5.7
10.501	2-Propanone, 1-hydroxy-	4.8
15.751	Glycolic acid, acetate	2.4
17.963	2-Propenyl, acetate	4.6
18.686	2-Cyclopenten-1-one	1.9
18.848	Furfural	2.0
24.596	2-Cyclopenten-1-one, 2-hydroxy	2.7
26.165	Furancarboxaldehyde, 5-methyl	1.6
27.350	2(5H)Furanone	2.1
31.389	Phenol	1.7
32.285	Guaiacol	3.3
33.840	2-Methyl phenol	1.0
37.243	4-Methyl guaiacol	4.1
40.960	Phenol, 2,6-Dimethyl	1.2
41.054	4-Ethyl guaiacol	1.3
43.592	4-Vinil guaiacol	3.9
44.648	3-(2-propenyl)guaiacol	1.4
49.262	4-(1-propenyl)guaiacol	3.8
49.790	Vanillin	1.0

*Only compounds with chromatographic peaks areas higher than 1% are listed.

28% of phenols. When MoO_3 was used as catalyst in the hydropyrolysis reaction, there was a complete suppression of the phenolic compounds with the corresponding formation of aromatic hydrocarbons. This result is in agreement with those reported by Prasomsri et al. [37] for the hydropyrolysis of lignin-derived model compounds using MoO_3 as catalyst. The authors propose that during the hydropyrolysis reaction MoO_3 undergoes a partial carburization forming oxy-carbide- and/or oxy-carbo-hydride-containing phases that would be responsible for the catalytic activity. However, the hypothesis that the deoxygenation takes place on oxygen vacancies created on MoO_3 through a reverse Mars-Van Krevelen reaction cannot be ruled out [38]. It is noteworthy

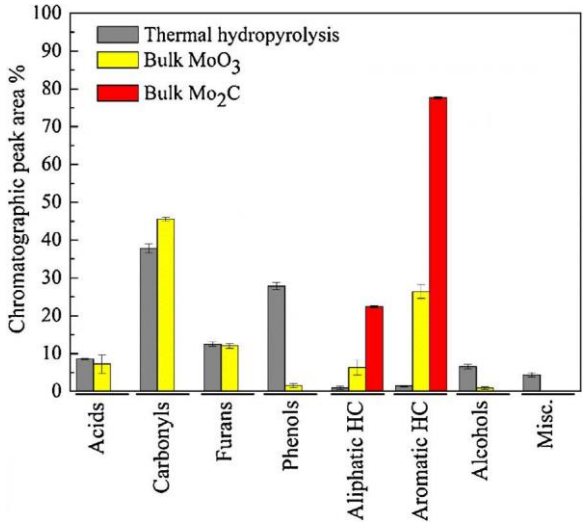

Fig. 3. Product distribution obtained in the biomass thermal hydropyrolysis and catalytic hydropyrolysis using bulk MoO_3 and bulk Mo_2C as catalysts.

that the amounts of acids, carbonyls and furans have remained broadly unchanged when compared with the thermal hydropyrolysis indicating that under the reaction conditions employed deoxygenation of phenols takes place preferentially.

Prasomsri et al. [37] have found that when treated in hydrogen flow at 400 °C, MoO_3 is active in the HDO of several oxygenated molecules (e.g. acetone, phenol, 2-hexanone, anisol, 2-methylfuran and 2,5-di-methylfuran) due to the oxygen vacancies formation. Our results show that only phenolic compounds were converted when MoO_3 was used as catalyst and the explanation for this can be related to the fact that in our case, the oxide was submitted to a thermal treatment under flow of He at 500 °C. In this way, the vacancies created in the MoO_3 lattice would occurs only during the reaction when hydrogen is present in the feed.

Significantly, the use of bulk Mo_2C as catalyst (Fig. 3) led to for-mation of hydrocarbons (aliphatics and aromatics) with no formation of other oxygenates such as acids, carbonyls, furans and phenols. This result indicates that Mo_2C was able to transform oxygenated com-pounds into aromatic and aliphatic hydrocarbons, showing an extensive hydro-deoxygenation degree, as previously demonstrated for HDO re-actions employing model molecules such as acetone [10,18], propanal [18], acetic acid [39], benzofuran [40] and a phenolic compound

Table 4
Main compounds produced in the thermal and catalytic hydropyrolysis of Canadian pinewood.

Compounds	Chromatographic peak area%									
	Thermal	MoO_3	Mo_2C	Al_2O_3	MoC/Al_2O_3	Pt/Al_2O_3	ZrO_2	MoC/ZrO_2	MgO	MoC/MgO
Acids										
Acetic acid	5.7	5.6	0	0	0	0	0	0	0	0
Others	2.6	0	0	0	0	0	0	0	0	0
Carbonyls										
Acetone	4.6	16.9	0	7.5	0	0	19.9	0	22.2	17.7
2-Butanone	0	4.0	0	1.6	0	0	9.4	0	10.2	3.5
Acetaldehyde	3.9	19.4	0	0	0	0	0	0	4.3	0
Linear ketones[a]	18.0	0.7	0	0	0	0	1.4	0	8.9	0.3
Cyclic ketones[b]	9.1	2.3	0	0.8	0	0	7.3	0	20.8	0.7
Others	2.5	0.9	0	0	0	0	0	0	4.1	
Furans										
Furfural	2.0	0	0	0	0	0	0	0	0	0
2(5H)Furanone	2.1	0	0	0	0	0	0	0	0	0
Furancarboxaldehyde, 5-methyl	1.6	0	0	0	0	0	0	0	0	0
Furan	0	8.7	0	13.5	0	0	2.9	0	5.7	0
2-Methyl furan	0.4	1.5	0	1.7	0	0	2.7	0	2.2	2.2
2,5-Dimethyl furan	0.1	0	0	0.6	0	0	0.4	0	0	1.3
Others	4.6	1.5	0	1.8	0	0	0.7		0.9	
Phenols										
Phenol	1.7	1.2	0	0.2	0	0	0.3	0	0.7	0
Guaiacol	3.3	0	0	0	0	0	0	0	0	0
Derived-guaiacol[c]	14.5	0	0	0	0	0	0	0	0	0
2-Methyl phenol	1.0	0.1	0	0.1	0	0	0.7	0	1.7	0.2
2,6-Dimethyl phenol	1.2	0	0	0	0		0.2	0	0.8	0
Others	5.3	0	0	0	0	0	0	0	0	0
Aliphatic HC										
C3	0	2.6	3.8	3.2	5.9	8.8	6.8	20.9	4.3	16.7
C4	0	5.0	11.8	6.9	14.9	25.6	5.4	14.4	4.5	9.4
C5	0	0	1.5	0	21.0	7.8	2.1	17.7	0	9.9
C6-C9	0.9	0.2	0.4	22.3	15.1	0	25.4	6.8	2.3	19.2
Aromatic HC										
Benzene	0.4	6.7	22.4	1.9	4.1	28.7	1.0	7.2	0.9	3.8
Toluene	0.5	10.0	28.6	4.9	5.9	17.5	1.9	10.9	1.9	4.4
1 aromatic ring[d]	0.3	8.7	18.6	28.4	26.2	6.7	15.6	18.2	3.8	11.2
2 aromatic rings[e]	0	1.3	8.1	2.9	6.9	4,9	0	3.9	0	0.7
Alcohols	6.5	0.8	0	0	0	0	0	0	0	0

[a] 2,3-Butanedione; 2-Pentanone; 3-Hexanone.
[b] Cyclopentanone; Cyclopentanone, 2-methyl-; 2-Cyclopenten-1-one, 2,3-dimethyl-.
[c] Guaiacol, 4-methyl-; Guaiacol, 4-ethyl-; Guaiacol, 4-vynil-; Guaiacol, 4-propyl-; Guaiacol, 3-(2-propenyl)-; Guaiacol, 4-(1-propenyl)-.
[d] Ethylbenzene; Xylene; Styrene; Benzene, dimethyl-; Benzene, trimethyl-; Indane; Benzene, 1-ethyl-2-methyl-.
[e] Naphthalene; Naphthalene, methyl-; Naphthalene, dimethyl-; Naphthalene, trimethyl-; Fluorene.

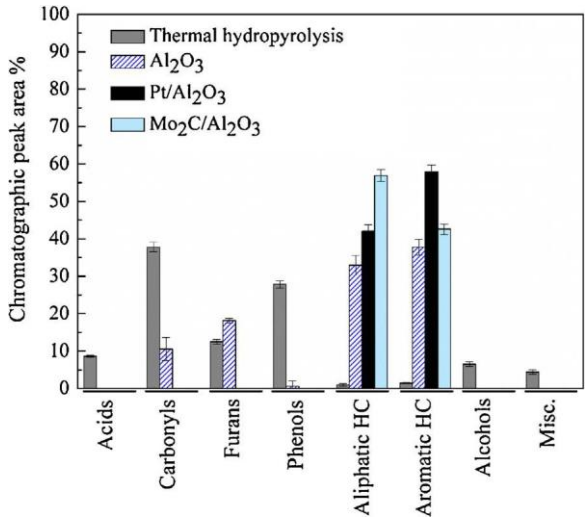

Fig. 4. Product distribution obtained in the biomass thermal hydropyrolysis and catalytic hydropyrolysis using Al_2O_3, 1.5 wt.% Pt/Al_2O_3 and MoC/Al_2O_3 as catalysts.

mixture (guaiacol, anisole, m-cresol, 1,2-dimethoxybenzene) [41]. Be-cause of the small amounts of catalyst used in the hydropyrolysis ex-periments, it was not possible to study the catalyst after the reaction to check out if part of the oxygenated compounds were transformed into coke.

As mentioned earlier, it is well known from the literature that car-bide catalysts have catalytic behavior similar to that of noble metal catalysts [9]. Thus, the 1.5 wt.% Pt/Al_2O_3 catalyst (characterization available in the Supplementary Information) was tested, in order to compare its product distribution to that of MoC/Al_2O_3 catalyst. The hydropyrolysis experiments were carried out under the same conditions and the results are presented in Fig. 4. The use of pure Al_2O_3 led to a suppression of the acids and phenols, 70% of carbonyls were converted and, interestingly, 77% of hydrocarbons were formed. This might be due to the dehydration of acids and phenols over the acid sites of Al_2O_3 [3]. Over Pt/Al_2O_3 catalyst, all the oxygenates were converted into aliphatic (42%) and aromatic (58%) HC. Promisingly, MoC/Al_2O_3 cat-alyst only produced aliphatic and aromatic hydrocarbons (57% and 43%, respectively), as well. Both Pt and MoC catalysts have the ability of complete deoxygenation and production of aliphatics, especially. In comparison, earlier report by Bridgewater [42] showed that total deoxygenation could be achieved over ZSM-5 but only (poly) aromatics were formed.

Comparatively, Pt/Al_2O_3 catalyst favored aromatic HC formation while MoC/Al_2O_3 catalyst promoted aliphatic formation. The difference in the amount of aromatics formed on Pt and MoC catalysts might be related to the acid sites of Al_2O_3, over which aromatization takes place [3]. As the loading of the active phases are quite different, it is rea-sonable to assume that alumina coverage was higher in the supported carbided catalyst, thus resulting on less acid sites from the Al_2O_3. The compounds produced over Pt/Al_2O_3 and MoC/Al_2O_3 catalysts are dis-played in Fig. 5 and it is noteworthy that the major aromatic com-pounds over Pt/Al_2O_3 catalyst were benzene and toluene, and the ali-phatic HC were C4 compounds (25 %). However, over MoC/Al_2O_3 catalyst, a variety of other aromatic compounds with one ring (26%) were produced, such as ethylbenzene and xylenes, and 37% of aliphatic HC corresponded to C5-C9 compounds which are the most compatible fuel components. Besides, both of them produced approximate amounts of compounds consisting of 2 aromatic rings, such as naphthalene and fluorene. As it is known, Al_2O_3 favors the polymerization reaction and coke formation, thus this result is in accordance with the literature [43].

The results presented in Figs. 4 and 5 clearly show that the MoC/ Al_2O_3 catalyst exhibited high reactivity for upgrading of hydropyrolysis

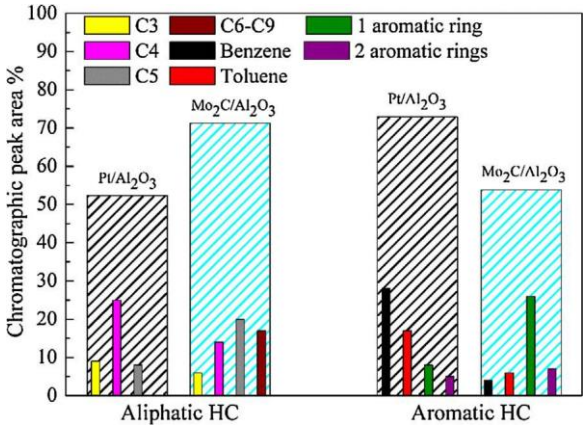

Fig. 5. Compounds produced during biomass catalytic hydropyrolysis using 1.5 wt.% Pt/ Al_2O_3 and MoC/Al_2O_3 as catalysts.

vapors. In order to investigate the effect of the acidity of the support over molybdenum carbide active phase performance in the hydro-pyrolysis of biomass, other supports were employed.

Figs. 4, 6 and 7 show that the acid-base properties of supports strongly influence the product distribution obtained during hydro-pyrolysis using carbide as active phase. In general, the acidity favored the production of aliphatic and aromatic hydrocarbons via dehydration reactions [3] and reduction of carbonyls compounds. On the other hand, the basic feature favored CeC coupling reactions (e.g. aldol-condensation, ketonization), which leads to the increasing of molecular chain, but not the removal of oxygen atom [44]. It is clearly observed that Al_2O_3, being the most acidic support, produced the highest per-centage of total HC (77%) and the lowest percentage of carbonyls (12%), while MgO, being the basic (less acidic) support, presented the opposite behavior (18% of total HC and 70% of carbonyls). As expected, the ZrO_2 support showed intermediate percentages of total hydro-carbons (52%) and carbonyls (40%), as it is an amphoteric material.

As can be seen in Table 4, hydrocarbon and carbonyl groups were produced by all supports, as well as furanic compounds, being furan the component present in the largest amount. Furthermore, phenolic spe-cies were also formed, but not in an appreciable quantity. Comparing with the thermal hydropyrolysis, it is noted that Al_2O_3, ZrO_2 and MgO reduced all the guaiacol derivatives, remaining only the phenolic ones such as phenol, 2-methyl phenol and 2,6-dimethyl phenol.

The incorporation of carbide to the supports promoted the pro-duction of more hydrocarbons than what was obtained for the bare

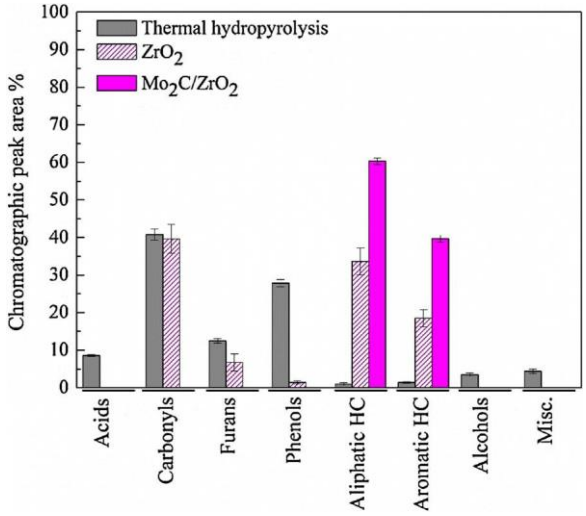

Fig. 6. Product distribution obtained in the biomass thermal hydropyrolysis and catalytic hydropyrolysis using ZrO_2 and MoC/ZrO_2 as catalysts.

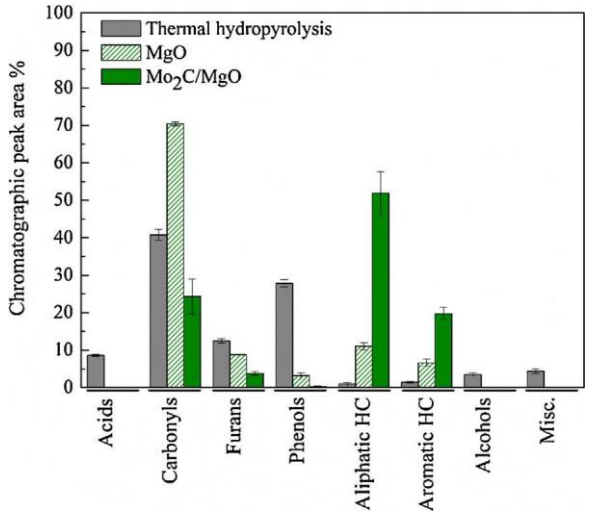

Fig. 7. Product distribution obtained in the biomass thermal hydropyrolysis and catalytic hydropyrolysis using MgO and MoC/MgO as catalysts.

supports, indicating that MoC was active in hydrodeoxygenation. Comparatively, it is observed that MoC/Al_2O_3 and MoC/ZrO_2 catalysts led to a complete deoxygenation of the hydropyrolysis vapors forming outputs with different compositions but consisting of hydrocarbons (60% and 40% of aromatics and aliphatics, respectively).

The MoC/ZrO_2 catalyst favored the formation of benzene and to-luene, corresponding to half of the total aromatic hydrocarbons formed. In contrast, these compounds represented only one quarter of the formed aromatics in MoC/Al_2O_3 catalyst. Amongst the aliphatic hy-drocarbons, MoC/ZrO_2 catalyst led to a major formation of C3 com-ponents (propane and propene), corresponding to one third (20%) of the total aliphatic compounds, whereas MoC/Al_2O_3 catalyst promoted the production of C5–C9 compounds.

One would expect that the more acidic catalyst (MoC/Al_2O_3) would lead to the highest formation of cracking products. When Table 4 is analyzed, it is clear that MoC/ZrO_2 showed the highest formation of C3 compounds (20.9%), whilst the most acidic catalyst (MoC/Al_2O_3) pre-sented a rather low formation of these kind of products (5.9%). This suggests that the formed C3 compounds observed for the MoC/ZrO_2 catalyst were not only formed by cracking reactions, but also by hy-drogenation of acetone formed during the hydropyrolysis of pinewood (thermal experiment). Moreover, the acetic acid presented in the vapor can undergo ketonization reaction, leading to the formation of more acetone and ZrO_2 was already reported as one of the best catalysts to perform this reaction [32]. Another important point to be considered is that on bare ZrO_2 there is the formation of a high amount of acetone (19.9%), then it is reasonable to assume that this ketone formed on the support could be hydrogenated to propane on the MoC sites, thus ex-plaining the high quantities of observed C3 products.

Analysis results presented in Fig. 7 reveals that not all oxygen was removed when MoC/MgO was used as catalyst. In this case, only 35% and 70% of the carbonyl and furan compounds were converted, re-spectively, although there was a complete conversion of acids, phenols and alcohols. The carbonyl compounds that remained were acetone (17%) and 2-butanone (3,5%), whereas the furans were 2-methylfuran (2.2%) and 2,5-dimethylfuran (1.3%). Moreover, this catalyst produced 72% of hydrocarbons, 51% of aliphatic species, which is a lower value than those obtained for MoC/Al_2O_3 and MoC/ZrO_2. Amongst the formed aliphatic HC, C5-C9 compounds appeared in major proportion (19%), whereas compounds with one aromatic ring, excluding benzene and toluene, were the most generated (11%) in the aromatic group.

The chemistry behind the reactions taking place during the thermal or catalytic pyrolysis reactions is quite complex and changes depending on the nature of the employed biomass. However, if the formed compounds are grouped into families an explanation of the role of the carburized species can be attempted. For instance, several works in the literature have shown that when molybdenum or tungsten carbide are used as catalysts in the hydrodeoxygenation of carboxylic acids [31,45–48] there is the hydrogenation of the carboxylic group, con-trarily to what is observed for noble metals, which promote dec-arbonylation and decarboxylation reactions. This behavior was ob-served in this work where the use of the molybdenum carbide has led to a suppression of the acids formed. However, in order to fully under-stand the role of the carbide active phase in the reaction networks in-volved and the interaction between the different families of compounds more fundamental studies using model molecules and mixtures of them are needed.

4. Conclusions

It is shown in this study that the MoC/Al_2O_3 catalyst showed high reactivity for upgrading of hydropyrolysis vapors, with its performance being comparable with 1.5 wt.% Pt/Al_2O_3. Thus, carbide-based catalyst is a promising alternative for the expensive (Pt) noble metal catalyst once they deoxygenated the pyrolysis vapors generated in the fast hy-dopyrolysis of Canadian pinewood to aliphatic and aromatic hydro-carbons, which are the most compatible fuel components. In addition, for the supported MoC catalysts, the acidity of the support influences the overall catalytic performance, leading to a larger formation of hy-drocarbons and to the deoxygenation of carbonyl compounds. Supported carbide catalysts studied here seem bifunctional. The sup-port have a definite role in the (inter)-conversion of fragments formed during pyrolysis via catalyzing dehydration, coupling (de)-alkylation and condensation reactions. Thus, the product pattern, aliphatics vs aromatics, can be manipulated by the choice of the support. Carbide catalysts show a satisfactory catalytic performance and, undoubtedly, are a potential alternative to replace noble metal in the hydropyrolysis of biomass to liquid fuels.

References

[1] J.C. Serrano-Ruiz, J.A. Dumesic, Catalytic routes for the conversion of biomass into liquid hydrocarbon transportation fuels, Energy Environ. Sci. 4 (2011) 83–99.
[2] M. Asadieraghi, W.M.A.W. Daud, H.F. Abbas, Heterogeneous catalysts for advanced bio-fuel production through catalytic biomass pyrolysis vapor upgrading: a review, RSC Adv. 5 (2015) 22234–22255.
[3] T.S. Nguyen, M. Zabeti, L. Lefferts, G. Brem, K. Seshan, Conversion of lig-nocellulosic biomass to green fuel oil over sodium based catalysts, Bioresour. Technol. 142 (2013) 353–360.
[4] A.V. Bridgwater, Review of fast pyrolysis of biomass and product upgrading, Biomass Bioenergy 38 (2012) 68–94.
[5] D.A. Ruddy, J.A. Schaidle, J.R. Ferrell III, J. Wang, L. Moens, J.E. Hensley, Recent advances in heterogeneous catalysts for bio-oil upgrading via ex situ catalytic fast pyrolysis: catalyst development through the study of model compounds, Green Chem. 16 (2014) 454–490.
[6] M. Zabeti, T.S. Nguyen, L. Lefferts, H.J. Heeres, K. Seshan, In situ catalytic pyrolysis of lignocellulose using alkali-modified amorphous silica alumina, Bioresour. Technol. 118 (2012) 374–381.
[7] P.M. Mortensen, J.D. Grunwaldt, P.A. Jensen, K.G. Knudsen, A.D. Jensen, A review of catalytic upgrading of bio-oil to engine fuels, Appl. Catal. A Gen. 407 (2011) 1–19.
[8] E.F. Mai, M.A. Machado, T.E. Davies, J.A. Lopez-Sanchez, V. Teixeira da Silva, Molybdenum carbide nanoparticles within carbon nanotubes as superior catalysts for γ-valerolactone production via levulinic acid hydrogenation, Green Chem. 16 (2014) 4092–4097.
[9] S. Ramanathan, S.T. Oyama, New catalysts for hydroprocessing: transition metal carbides and nitrides, J. Phys. Chem. 99 (1995) 16365–16372.
[10] M.M. Sullivan, A. Bhan, Acetone hydrodeoxygenation over bifunctional mettalic-acidic molybdenum carbide catalysts, Am. Chem. Soc. Catal. 6 (2016) 1145–1152.
[11] R. Ma, K. Cui, L. Yang, X. Ma, Y. Li, Selective catalytic conversion of guaiacol to phenols over a molybdenum carbide catalyst, Chem. Commun. 51 (2015) 10299–10301.

[12] P.M. Mortensen, H.W.P. De Carvalho, J.D. Grunwaldt, P.A. Jensen, A.D. Jensen, Activity and stability of Mo_2C/ZrO_2 as catalyst for hydrodeoxygenation of mixtures of phenol and 1-octanol, J. Catal 328 (2015) 208–215.

[13] E. Santillan-Jimenez, M. Perdu, R. Pace, T. Morgan, M. Crocker, Activated carbon, carbon nanofiber and carbon nanotube supported molybdenum carbide catalysts for the hydrodeoxygenation of guaiacol, Catalysts 5 (2015) 424–441.

[14] W.S. Lee, Z. Wang, R.J. Wu, A. Bhan, Selective vapor-phase hydrodeoxygenation of anisole to benzene on molybdenum carbide catalysts, J. Catal. 319 (2014) 44–53.

[15] S. Li, N. Li, G. Li, A. Wang, Y. Cong, X. Wang, T. Zhang, Synthesis of diesel range alkanes with 2-methylfuran and mesityl oxide from lignocellulose, Catal. Today 234 (2014) 91–99.

[16] S. Boullosa-Eiras, R. Lødeng, H. Bergem, M. Stöcker, L. Hannevold, E.A. Blekkan, Catalytic hydrodeoxygenation (HDO) of phenol over supported molybdenum car-bide nitride, phosphide and oxide catalysts, Catal. Today 223 (2014) 44–53.

[17] H. Ren, Y. Chen, Y. Huang, W. Deng, D.G. Vlachos, J.G. Chen, Tungsten carbides as selective deoxygenation catalysts: experimental and computational studies of con-verting C3 oxygenates to propene, Green Chem. 16 (2014) 761–769.

[18] H. Ren, W. Yu, M. Salciccioli, Y. Chen, Y. Huang, K. Xiong, D.G. Vlachos, J.G. Chen, Selective hydrodeoxygenation of biomass-derived oxygenates to unsaturated hy-drocarbons using molybdenum carbide catalysts, ChemSusChem 6 (2013) 798–801.

[19] M.A. Patel, M.A.S. Baldanza, V. Teixeira da Silva, A.V. Bridgwater, In situ catalytic upgrading of bio-oil using supported molybdenum carbide, Appl. Catal. A Gen. 458 (2013) 48–54.

[20] J.S. Choi, A.H. Zacher, H. Wang, M.V. Olarte, B.L. Armstrong, H.M. Meyer, I.I. Soykal, V. Schwartz, Molybdenum carbides, active and in situ regenerable cat-alysts in hydroprocessing of fast pyrolysis bio-oil, Energy Fuels 30 (2016) 5016–5026.

[21] F.L.P. Resende, Recent advances on fast hydropyrolysis of biomass, Catal. Today 269 (2015) 148–155.

[22] J.S. Lee, S.T. Oyama, M. Boudart, Molybdenum carbide catalysts I. Synthesis of unsupported powders, J. Catal 106 (1987) 125–133.

[23] A.S. Rocha, A.B. Rocha, V. Teixeira da Silva, Benzene adsorption on Mo_2C: A the-oretical and experimental study, Appl. Catal. A Gen. 379 (2010) 54–60.

[24] K. Koichumanova, A.K.K. Vikla, D.J.M. De Vlieger, K. Seshan, B.L. Mojet, L. Lefferts, Towards stable catalysts for aqueous phase conversion of ethylene glycol for re-newable hydrogen, ChemSusChem 6 (2013) 1717–1723.

[25] V.L.S. Teixeira da Silva, M. Schmal, S.T. Oyama, Niobium carbide synthesis from niobium oxide: study of the synthesis conditions, kinetics, and solid-state trans-formation mechanism, J. Solid State Chem. 123 (1996) 168–182.

[26] C.Q. Dong, Z.F. Zhang, Q. Lu, Y.P. Yang, Characteristics and mechanism study of analytical fast pyrolysis of poplar wood, Energy Convers. Manag. 57 (2012) 49–59.

[27] J. Grams, M. Niewiadomski, A.M. Ruppert, W. Kwapiński, Influence of Ni catalyst support on the product distribution of cellulose fast pyrolysis vapors upgrading, J. Anal. Appl. Pyrolysis 113 (2015) 557–563.

[28] M.J. Jeon, J.K. Jeon, D.J. Suh, S.H. Park, Y.J. Sa, S.H. Joo, Y.K. Park, Catalytic pyrolysis of biomass components over mesoporous catalysts using Py-GC/MS, Catal. Today 204 (2013) 170–178.

[29] P. Kaewpengkrow, D. Atong, V. Sricharoenchaikul, Effect of Pd, Ru, Ni and ceramic supports on selective deoxygenation and hydrogenation of fast pyrolysis Jatropha residue vapors, Renew. Energy 65 (2014) 92–101.

[30] P. Kaewpengkrow, D. Atong, V. Sricharoenchaikul, Catalytic upgrading of pyrolysis vapors from Jatropha wastes using alumina, zirconia and titania based catalysts, Bioresour. Technol. 163 (2014) 262–269.

[31] L.A. Sousa, J.L. Zotin, V. Teixeira da Silva, Hydrotreatment of sunflower oil using supported molybdenum carbide, Appl. Catal. A Gen. 449 (2012) 105–111.

[32] T.N. Pham, T. Sooknoi, S.P. Crossley, D.E. Resasco, Ketonization of carboxylic acids: mechanism, catalysts, and implications for biomass concersion, Am. Chem. Soc. Catal. 3 (2013) 2456–2473.

[33] S.K. Bej, C.A. Bennett, L.T. Thompson, Acid and base characteristics of molybdenum carbide catalysts, Appl. Catal. A Gen. 250 (2003) 197–208.

[34] A.M. Azeez, D. Meier, J. Odermatt, T. Willner, Fast pyrolysis of African and European lignocellulosic biomasses using Py-GC/MS and fluidized bed reactor, Energy Fuels 24 (2010) 2078–2085.

[35] C. Mukarakate, X. Zhang, A.R. Stanton, D.J. Robichaud, P.N. Ciesielski, K. Malhotra, B.S. Donohoe, E. Gjersing, R.J. Evans, D.S. Heroux, R. Richards, K. Iisa, M.R. Nimlos, Real-time monitoring of the deactivation of HZSM-5 during upgrading of pine pyrolysis vapors, Green Chem. 16 (2014) 1444–1461.

[36] S. Vichaphund, D. Aht-ong, V. Sricharoenchaikul, D. Atong, Catalytic upgrading pyrolysis vapors of Jatropha waste using metal promoted ZSM-5 catalysts: an analytical PY-GC/MS, Renew. Energy 65 (2014) 70–77.

[37] T. Prasomsri, M. Shetty, K. Murugappan, Y. Roman-Leshkov, Insights into the cat-alytic activity and surface modification of MoO_3 during the hydrodeoxygenation of lignin-derived model compounds into aromatic hydrocarbons under low hydrogen pressures, Energy Environ. Sci. 7 (2014) 2660–2669.

[38] T. Prasomsri, T. Nimmanwudipong, Y. Roman-Leshkov, Effective hydro-deoxygenation of biomass-derived oxygenates into unsaturated hydrocarbons by MoO_3 using low H_2 pressures, Energy Environ. Sci. 6 (2013) 1732–1738.

[39] J.A. Schaidle, J. Blackburn, C.A. Farberow, C. Nash, K.X. Steirer, J. Clark, D.J. Robichaud, D.A. Ruddy, Experimental and computational investigation of acetic acid deoxygenation over oxophilic molybdenum carbide: surface chemistry and active site identity, Am. Chem. Soc. Catal. 6 (2016) 1181–1197.

[40] B. Dhandapani, T. St Clair, S.T. Oyama, Simultaneous hydrodesulfurization hy-drodeoxygenation, and hydrogenation with molybdenum carbide, Appl. Catal. A Gen. 168 (1998) 219–228.

[41] C.J. Chen, W.S. Lee, A. Bhan, Mo_2C catalyzed vapor phase hydrodeoxygenation of lignin-derived phenolic compound mistures to aromatics under ambient pressure, Appl. Catal. A Gen. 510 (2016) 42–48.

[42] A. Bridgewater, Biomass fast pyrolysis, Therm. Sci. 8 (2004) 21–50.

[43] R. Feng, S. Liu, P. Bai, K. Qiao, Y. Wang, H.A. Al-Megren, M.J. Rood, Z. Yan, Preparation and characterization of γ-Al_2O_3 with rich brønsted acid sites and its application in the fluid catalytic cracking process, J. Phys. Chem. C 118 (2014) 6226–6234.

[44] E.F. Iliopoulou, Review of C-C coupling reactions in biomass exploitation processes, Curr. Org. Synth. 7 (2010) 587–598.

[45] S.A.W. Hollak, R.W. Gosselink, D.S. van Es, J.H. Bitter, Comparison of tungsten and molybdenum carbide catalysts for the hydrodeoxygenation of oleic acid, ACS Catal. 3 (2013) 2837–2844.

[46] D.R. Stellwagen, J.H. Bitter, Structure–performance relations of molybdenum and tungsten carbide catalysts for deoxygenation, Green Chem. 17 (2015) 582–593.

[47] R.W. Gosselink, S.A.W. Hollak, S.W. Chang, J. van Haveren, K.P. de Jong, J.H. Bitter, D.S. van Es, Reaction pathways for the deoxygenation of vegetable oils and related model compounds, ChemSusChem 6 (2013) 1576–1594.

[48] R.W. Gosselink, D.R. Stellwagen, J.H. Bitter, Tungsten-based catalysts for selective deoxygenation, Angew. Chem. Int. Ed. Engl. 52 (2013) 5089–5092.